CHAPTER-3

ELECTRONIC TRANSPORT IN GRAPHENE SYSTEMS AT FINITE TEMPERATURE

In this chapter we report our theoretical calculations on the temperature and carrier dependent conductivity (σ) of doped Graphene systems- monolayer (MLG), bilayer (BLG) and monolayer gapped Graphene (MLGG) within the framework of Boltzmann transport formalism. Since screening effects have known to be of vital importance in explaining the σ of Graphene systems therefore we first worked out the behaviour of the temperature dependent polarization function for Graphene systems. The polarization function of MLG has a local minimum near $T \approx 0.45T_f$ for $q < 2k_f$, however it increases monotonically for $q \geq 2k_f$. Wherein the case of BLG, polarization function has a sharp peak at $q = 2k_f$ for $T = 0$ K and the height of peak at $q = 2k_f$ strongly suppressed as temperature increases. Moreover polarization function of MLGG has been compared with that of MLG, BLG and 2DEG to see the effects of gap. It is found that the MLGG polarization function exhibits a strong dependence on temperature, wave vector and band gap and the effect translates to the σ of MLGG. The nature of temperature dependent σ in Graphene systems is observed to be non-monotonic, decreasing with temperature at low temperatures, and increasing at high temperatures. For $T \ll T_f$, MLG has poor quadratic temperature dependence metallic nature, BLG has strong linear temperature dependence metallic nature and MLGG has both, poor metallic nature for $a(= 0, 0.3 \,\&\, 0.6)$ and strong metallic nature at $a = 0.9$. We also obtained numerical results of temperature dependent σ of MLGG as a function of carrier concentration which shows linear behaviour as observed experimentally, and also shows an increase in magnitude with the increase in temperature and decrease in magnitude with the increase in

band gap. We also find that the σ computed as a function of temperature by averaging over quasi-particle energy significantly differs from that computed at Fermi energy, suggesting that a notable contribution to temperature dependent σ is made by electrons close to the Fermi level.

3.1 Introduction

Temperature and density dependent transport properties of Graphene systems (i.e. MLG, BLG and MLGG) have been great interest at fundamental and technological efforts [1]. In the previous chapter 2, we have reported our results on electron-impurity scattering rate of Graphene systems at zero temperature. However, resent experimental works on the conductivity/resistivity of Graphene systems are carried out at finite temperature (low temperature or room temperature). Moreover temperature dependent conductivity $(\sigma(T))$ provides fundamental knowledge like- in which temperature range system show metallic or insulating behaviour and at what temperature phase transition occur. This fundamental knowledge makes Graphene promising material for Graphene based high performance sensors and devices.

The charge transport in MLG, BLG and MLGG display novel chirality that has attracted much theoretical and experimental attention [2-9] due to different energy dispersion relation and chiral nature. Charge transport in Graphene systems sharply differ from that of 2DEG observed in doped semiconductor heterostructures [8-9]. The BLG shows energy dispersion similar to that of 2DEG while, the linear nature of carrier density dependence of conductivity $(\sigma(n))$ in BLG is similar to that observed in MLG at zero temperature. There has been substantial recent experimental and theoretical work on both density and temperature dependence transport properties of MLG [1, 8, 10-12] and BLG [9, 13-17]. Theoretically calculated $\sigma(T)$ of MLG manifest metallic (semiconducting) temperature-

dependent conductivity for $T \ll T_f$ $(T \gg T_f)$ where T_f is Fermi temperature [8]. Similar nature of $\sigma(T)$ also observed in the BLG and regular parabolic 2D electron gas (2DEG) system with strong linear temperature dependence while MLG has a weak quadratic temperature dependence [9]. Various theories of charge transport in Graphene systems appear to suggest that σ obtained by considering a scattering mechanism based on screened charged impurities in Boltzmann equation agrees with the experimental results. The intrinsic parameters that govern σ and electron-impurity scattering rate $(\hbar/\tau)$ in MLG, BLG and MLGG are quasi particle energy (E), temperature (T) and carrier concentration (n_c), and additionally energy gap (Δ) in BLG and MLGG. Theoretical understanding of σ requires detailed investigations on how polarization function (Π) and σ depends on q, T and Δ. There have been several calculations of the polarization function and its properties for MLG, BLG and MLGG [4, 5, 8, 9, 18-24]. Also the σ as a function of various influencing parameters for MLG, BLG and MLGG has been reported in several publications [3, 4, 6- 9, 22].

In this chapter, we report our theoretical investigations on Graphene systems polarization function, Graphene systems σ and its dependence on various governing intrinsic parameters like E, T , n_c and Δ. The σ in Graphene systems has been dealt within the Boltzmann transport theoretical approach. Most of the existing theoretical studies on MLGG have been performed by calculating static and dynamical polarization functions at zero temperature and zero magnetic field [22-29]. In the calculation of σ at $T = 0$ K, all the charge carriers are at the Fermi level and the averaging of the relaxation time over entire energy range can be ignored. At finite temperature the carrier concentration is expressed in terms of Fermi distribution function therefore the relaxation time should be taken as the average of the relaxation time of individual charge carriers. Therefore, it is not appropriate to ignore the averaging, since τ at Fermi level can significantly differ from $\langle\tau\rangle$ particularly at moderate and high temperatures. The main motive of our work reported in this chapter has been to

investigate how the polarization function of Graphene systems and hence the σ varies with T, n_c and Δ. Also, at very low temperatures, the Fermi function behaves like step function and hence there is no significant difference between σ computed by averaging over E and σ computed at Fermi energy. However, as temperature increases, σ computed by averaging over E significantly differs from that computed at Fermi energy. Hence, the σ computed by averaging over E and not the σ at Fermi energy describe the experimental results more accurately.

3.2 Formalism

In terms of the average relaxation time $\langle \boldsymbol{\tau} \rangle$, the temperature dependent $\boldsymbol{\sigma}(\boldsymbol{T})$ for Graphene systems within the Boltzmann transport formalism can be expressed as [2];

$$\sigma(T) = (be^2/h)\left(E_f \langle \tau \rangle/\hbar\right) \tag{3.1}$$

where $\langle \tau \rangle$ is the average value of τ over all possible values of quasiparticle energy, E_{sk} . b is 2 for MLG and MLGG, and is 4 for BLG. The energy averaged finite temperature scattering time is given by [2],

$$\langle \tau \rangle = \int E\, \tau(E, \mathrm{T}) \left(-\frac{\partial f}{\partial E}\right) dE \Big/ \int E \left(-\frac{\partial f}{\partial E}\right) dE. \tag{3.2}$$

Where $f(E) = 1/\left(1 + e^{((E-\mu_c)\beta)}\right)$ is the Fermi distribution function, $\tau(E,T)$ is the finite temperature and energy dependent scattering time of an electron scattered by disorder or statically screened Coulomb potential, given by [8, 9]

$$\frac{\hbar}{\tau(E,T)} = 2\pi n_i \int \frac{d^2k'}{(2\pi)^2} \left|\frac{v_i(q)}{\epsilon(q,T)}\right|^2 (1 - \cos\theta_{kk'})\, F(\boldsymbol{k}, \boldsymbol{k}')\, \delta(E_{sk} - E_{sk'}). \tag{3.3}$$

Where n_i is the concentration of impurity centers, $\theta_{kk'}$ is the scattering angle between the scattering in and out wave vectors $\boldsymbol{k}$ and $\boldsymbol{k}'$, $v_i(q) = 2\pi e^2/\kappa q$ is the two dimensional Fourier transform of the bare charge impurity Coulomb potential, where e is the electronic

charge, κ is the average background dielectric constant ($\approx$ 5.5 (4.0) for Graphene placed on SiC (SiO_2) with other side being exposed to air), $q = |\boldsymbol{k} - \boldsymbol{k}'| = 2\,(E/\gamma)\,\sin(\theta/2)$ is the momentum transferred to a scattered electron, $F(\boldsymbol{k}, \boldsymbol{k}')$ is the chirality function and it is defined in chapter 2. In Eq. (3.3), $\epsilon(q,T)$ is temperature dependent static dielectric function, which within linear response theory is given by

$$\epsilon(q,T) = 1 + V(q)\Pi(q,T), \tag{3.4}$$

where $\Pi(q,T)$ is the temperature dependent polarization function. The temperature dependent polarization function is an important quantity in calculating scattering rate of screened electron gas at finite temperature. The polarization function for the cases of both doped and undoped Graphene systems have been calculated at zero temperature [4, 5, 22, 23, 28] as well as at finite temperature [8, 9, 24] in the recent past. The effect of band gap on the ground state properties of Dirac electrons in a doped Graphene at zero temperature has also been studied [22]. We present here the detailed analysis of the numerically computed temperature dependent polarization function for MLGG and its comparison with that of MLG and BLG. Earlier, analytical results have been presented only in the asymptotic limits and detailed analysis of the polarization function at all q-values as well as temperature and gap values are missing [24]. The temperature dependent polarization function for MLG, BLG and MLGG in the random phase approximation (RPA) is given by [8, 9, 24],

$$\frac{\Pi^{\mathrm{MLG}}(q,T)}{N^{\mathrm{MLG}}(E_f)} = \frac{\mu_c}{E_f} + \frac{\pi}{8}\frac{q}{k_f} + \frac{2T}{T_f}\ln\left(1 + e^{-\beta\mu_c}\right) - \int_0^{\frac{q}{2}} \frac{dk}{k_f}\left(\frac{\sqrt{1-(2k/q)^2}}{1+e^{\beta(E_k-\mu_c)}} + \mu_c \to -\mu_c\right), \tag{3.5}$$

$$\frac{\Pi^{\mathrm{BLG}}(q,T)}{N^{\mathrm{BLG}}(E_f)} = \int_0^{\infty} \frac{dk}{k^3}\left\{\sqrt{4k^4+q^4} - k^2 - |k^2-q^2| - \left(\frac{1}{1+e^{\beta(E_k-\mu_c)}} + \mu_c \to -\mu_c\right)\right.$$
$$\left. \times \left(2k^2 - \sqrt{4k^4+q^4} + \frac{\left(2k^2-q^2\right)^2}{q\sqrt{q^2-4k^2}}\theta(q-2k)\right)\right\} \tag{3.6}$$

and

$$\frac{\Pi^{\mathrm{MLGG}}(q,T)}{N^{\mathrm{MLGG}}(\mu_f)} = \frac{\mu_c}{2\,\mu_f} - \frac{\Delta}{\mu_f} + \frac{1}{\beta}\left(\ln\left[1 + e^{-\beta(\mu_c - \Delta)}\right] + \Delta \to -\Delta\right) - \frac{\gamma^2}{q\,\mu_f}\left\{\int_0^{\frac{q}{2}} \frac{k\,dk}{\sqrt{\gamma^2 k^2 + \Delta^2}}\right.$$

$$\left.\times\left(\sqrt{\frac{q^2\gamma^2}{4} - \gamma^2 k^2} - \frac{2\Delta^2}{\sqrt{\frac{q^2\gamma^2}{4} - \gamma^2 k^2}}\right)\left(\frac{1}{1+e^{\beta\left(\sqrt{\gamma^2 k^2 + \Delta^2} - \mu_c\right)}} + \mu_c \to -\mu_c\right)\right\}. \qquad (3.7)$$

Here μ_c is the finite temperature chemical potential determined by the conservation of the total electron density (see Appendix-C) and $N^{\mathrm{MLG}}(E_f)$, $N^{\mathrm{BLG}}(E_f)$ and $N^{\mathrm{MLGG}}(\mu_f)$ are the density of state at Fermi level of MLG, BLG and MLGG respectively define in chapter 2. The Eq. (3.7) yields the prior reported results [8, 18, 25] for polarization function at $T = 0\mathrm{K}$ for MLGG and at finite temperature for MLG when $\Delta/\mu_f = a = 0$. Substituting Eqs. (3.5), (3.6) & (3.7) into Eq. (3.3), and then simplifying the integrals, we obtain finite temperature scattering rate for MLG, BLG and MLGG respectively;

$$\frac{\hbar}{\tau^{\mathrm{MLG}}(E,T)} = 4n_i N^{\mathrm{MLG}}(E)\int_0^{\pi} \mathrm{d}\theta \left(\frac{\pi \mathrm{e}^2}{\kappa q\, \epsilon^{\mathrm{MLG}}(q,T)}\right)^2 (1-\cos\theta)\ (1+\cos\theta) \qquad (3.8)$$

$$\frac{\hbar}{\tau^{\mathrm{BLG}}(E,T)} = 4n_i N^{\mathrm{BLG}}(E)\int_0^{\pi} \mathrm{d}\theta \left(\frac{\pi \mathrm{e}^2}{\kappa q\, \epsilon^{\mathrm{BLG}}(q,T)}\right)^2 (1-\cos\theta)\ (1+\cos 2\theta) \qquad (3.9)$$

and

$$\frac{\hbar}{\tau^{\mathrm{MLGG}}(E,T)} = 4n_i N^{\mathrm{MLGG}}(E)\int_0^{\pi} \mathrm{d}\theta \left(\frac{\pi \mathrm{e}^2}{\kappa q\, \epsilon^{\mathrm{MLGG}}(q,T)}\right)^2 (1-\cos\theta)\left(\left(\frac{E^2+2\Delta^2}{E^2+\Delta^2}\right) + \left(\frac{E^2}{E^2+\Delta^2}\right)\cos\theta\right) \qquad (3.10)$$

Where, the factor $(1-\cos\theta)$ which is invariably present in the Boltzmann transport equation weighs the amount of backward scattering of the electrons by impurity. for $\Delta = 0$, factor $\left(\left(\frac{E^2+2\Delta^2}{E^2+\Delta^2}\right) + \left(\frac{E^2}{E^2+\Delta^2}\right)\cos\theta\right)$ in Eq. (3.10) reduces to $(1+\cos\theta)$ that suppresses the large angle scattering in MLG. However, in case of MLGG there is breaking of the sub lattice symmetry because of the bandgap, which contributes to the large angle scattering with

increasing band gap. At lower temperatures, the derivative of Fermi distribution function, $\partial f/\partial E_k$ behaves like step function and therefore it is assumed that for all practical purposes there should not be any significant difference in temperature dependent σ calculated at Fermi energy or with the use of Eq. (3.1).

Rest of the chapter, we used following scaled parameters: $a = \Delta/\mu_f$, $\alpha = 4e^2/(\gamma\kappa)$ (dimensionless coupling constant used in MLG and MLGG, which has value ≈ 1 (& 2) for Graphene sheets on SiC (BN) substrate), $\beta = 4\,m\,e^2/\left(\hbar^2\,k\,k_f\right)$ with $m \approx 0.033m_e$ (dimensionless coupling constant used in BLG, which has value ≈ 4.3 (& 5.6) for BLG on SiC (SiO_2) substrate and $n_c = 10^{12}$ cm^{-2}) and $N = n_c/n_i$ (the scaled carrier concentration). The normalized conductivity at finite T for Graphene systems is then obtained from the ratio; $\sigma(T)/\sigma(T=0) = \tau(T)/\tau(T=0)$, where $\tau(T=0)$ has been computed by taking $T = 0$ in Eq. (3.3).

3.3 Results & Discussions

3.3.1 Temperature Dependent Polarization Function of MLG, BLG & MLGG

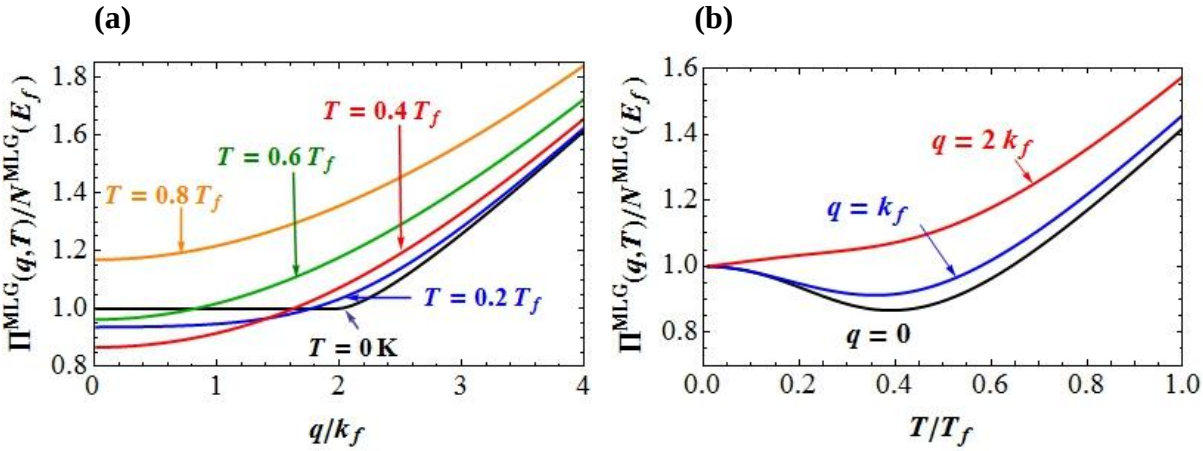

Figure 3.1: Temperature dependent MLG polarization function (a) as a function of wave vector for different values of temperature and (b) as a function of temperature for different values of wave vector.

In Figure 3.1 we show the finite-temperature $\Pi^{\mathrm{MLG}}(q,T)$ of MLG calculated using Eq. (3.5) (a) for different temperatures as a function of wave vector, and (b) for different wave vectors as a function of temperature. The $\Pi^{\mathrm{MLG}}(q,T)$ function has a local minimum near $T \approx 0.45T_f$ for $q < 2k_f$, however it increases monotonically for $q \geq 2k_f$, which arises from the excitation of electrons from the valence band to the conduction band. The different temperature dependence between small wave vectors $(q < 2k_f)$ and large wave vectors $(q > 2k_f)$ gives rise to very different temperature dependent scattering rates MLG. From Figure 3.1 (b), the $\Pi^{\mathrm{MLG}}(q,T)$ initially decline with increasing of T up to the $T \approx 0.45T_f$ for $q = 0$ and $q = k_f$ and there after it increases with increasing of T. Since the $\Pi^{\mathrm{MLG}}(q,T)$ at $q = 2k_f$ increases monotonically with T, the $\sigma(T)$ caused by $q = 2k_f$ scattering increases with increasing T. In Graphene, since the most dominant scattering happens at q~$k_f$we have to investigate the temperature dependent $\Pi^{\mathrm{MLG}}(q,T)$ at $q \sim k_f$, which decreases with temperature (for $T \ll T_f$) and gives rise to the decreases in σ with temperature as observed experimentally.

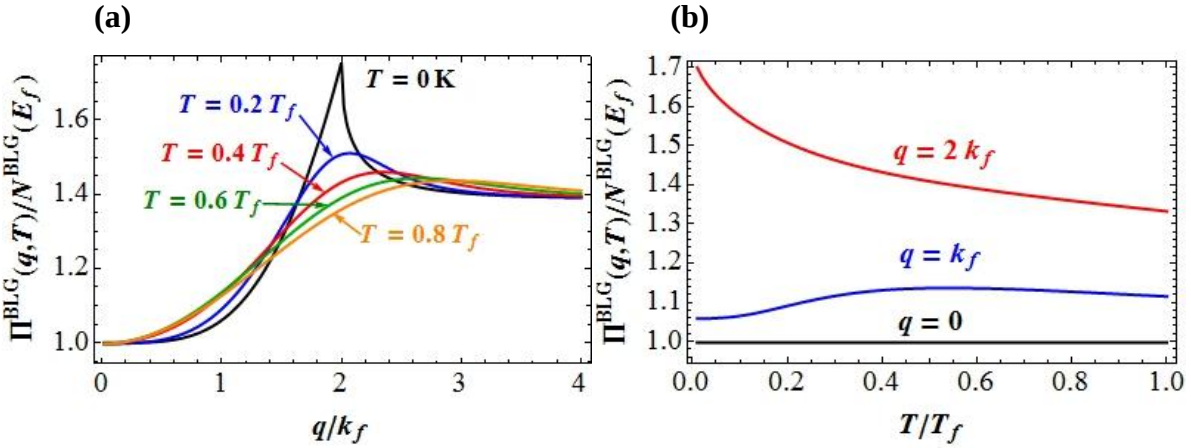

Figure 3.2: Temperature dependent BLG polarization function (a) as a function of wave vector for different values of temperature and (b) as a function of temperature for different values of wave vector.

In Figure 3.2 (a), we show $\Pi^{\mathrm{BLG}}(q,T)$ of BLG as a function of q for different values of T calculated using Eq. (3.6). The $\Pi^{\mathrm{BLG}}(q,T)$ shows weak temperature dependence in all the wave-vector regimes except for $q = 2k_f$. The $\Pi^{\mathrm{BLG}}(q,T)$ increases monotonically with q in the regime $[0,2k_f]$ and monotonically decreasing in the regime $q > 2k_f$. We observe a sharp peak at $q = 2k_f$ for $T = 0$ K due to the backward scattering arising from the chirality. The height of peak in $\Pi^{\mathrm{BLG}}(q,T)$ at $q = 2k_f$ strongly suppressed as temperature increases. M. Lv and S. Wan [9] theoretically investigated that $\Pi^{\mathrm{BLG}}(q,T)$ approaches a constant value $N^{\mathrm{BLG}} \log 4$, arising from the fact that the interband transition dominates over the intraband contribution in the large wave-vector regime $(q \gg 2k_f)$. We also observed strong T dependence of the $\Pi^{\mathrm{BLG}}(q,T)$ at $q = 2k_f$ and consequently the BLG would have a anomalously strong $\sigma(T)$ for $T \ll T_f$. For more detail study, we also plotted $\Pi^{\mathrm{BLG}}(q,T)$ as a function of T for different values of q. $\Pi^{\mathrm{BLG}}(q,T)$ show a constant value for all temperatures at $q = 0$, nonmonotonic behavior at $q = k_f$ and monotonically decreases with increasing of temperature at $q = 2k_f$. One novel phenomenon is that at $q = 0$, the $\Pi^{\mathrm{BLG}}(q,T)$ equals to a constant value for all temperatures, i.e., $\Pi(q = 0,T) = N^{\mathrm{BLG}}(E_f)$ which is very different from that of MLG, where the polarizability $\Pi^{\mathrm{MLG}}(q = 0,T)$ shows a nonmonotonic behavior. The reason is, at $q = 0$, the intraband transition polarization $\Pi_{\mathrm{Intra}}(q = 0,T) = N^{\mathrm{BLG}}(E_f)$ while the interband transition polarization $\Pi_{\mathrm{Inter}}(q = 0,T) = 0$, i.e., the interband transition is forbidden at zero momentum transfer for all temperatures in BLG.

Variation in polarization function $\left(\Pi^{\mathrm{MLGG}}(q,T)\right)$ of MLGG with wave vector at larger gap value $a(= 0.9 \,\&\, 0.99)$ and at low temperatures is shown in Figures 3.3(a) & 3.3(b). The sharp decline seen in $\Pi^{\mathrm{MLGG}}(q,T)$ from a constant value at $q = 2k_f$ and $T = 0$ K, changes to a smooth variation on increasing the temperature. This abrupt decline in $\Pi^{\mathrm{MLGG}}(q,T)$ at

$q = 2k_f$ is associated with Friedel oscillations, which at finite and reasonably higher temperatures wash out.

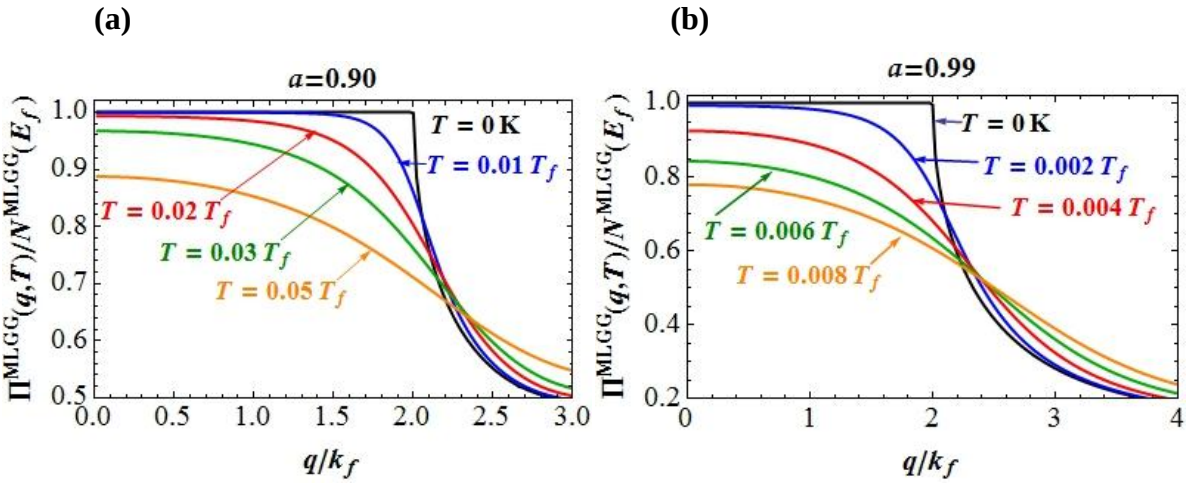

Figure 3.3: Figures (a) and (b) show the wave-vector dependence of polarization function for different values of temperature at gap values of $a = 0.9$, and 0.99 respectively. The curves in this case are similar to polarization function for a Si(001) inversion layer with 2×10^{12} electron per cm^2 [30-31].

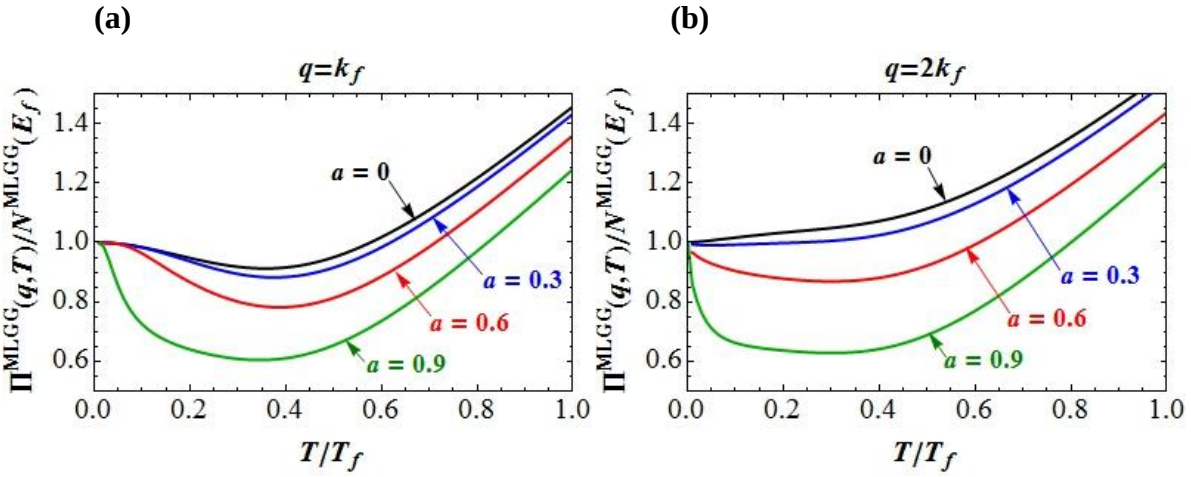

Figure 3.4: Temperature dependent polarization function for different gap values at; (a) $q = k_f$ and (b) $q = 2k_f$.

The computed $\Pi^{\mathrm{MLGG}}(q,T)$ as a function of temperature using Eq. (3.10) for different values of $a(= 0.0, 0.3, 0.6 \,\&\, 0.9)$ at two values of $q\left(= k_f \,\&\, 2k_f\right)$ are plotted in Figures 3.4(a) & 3.4(b). A slight change (decrease) in nature of $\Pi^{\mathrm{MLGG}}(q,T)$ versus wave vector curve can be

noticed on enhancing q from k_f to $2k_f$. Also, as can be noticed from the figures, the $\Pi^{\mathrm{MLGG}}(q,T)$ first declines with temperature and after hitting a minimum increases almost linearly for all nonzero values of a. A reverse trend observed at higher temperatures compared to that at low temperature regime is indicative of phase transition taking place in MLGG.

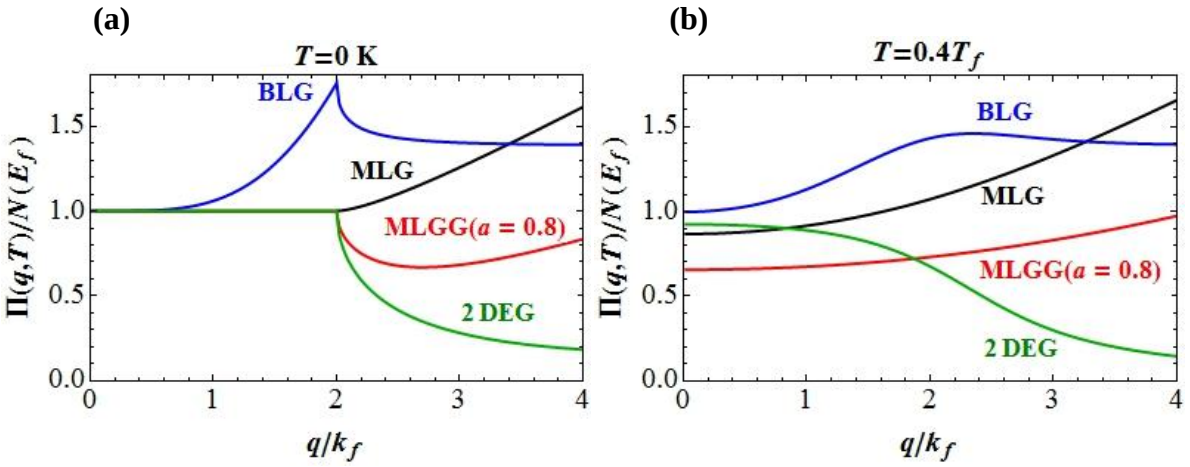

Figure 3.5: Comparative plot of polarization function of MLG, BLG, MLGG & 2DEG at zero and finite temperature ($T = 0.4T_f$) are shown in Figures 3.5(a) and 3.5(b), respectively.

Finally in Figures 3.5(a) & 3.5(b) the comparative plot of the polarization function of MLG, MLGG, BLG & 2DEG are shown at zero and finite temperature ($T = 0.4T_f$), respectively. The interplay of linear energy band dispersion relation, chirality, bandgap and temperature endow MLGG with overall strange screening properties which are a mixture of MLG, BLG and 2DEG screening properties. It is known that MLG also exhibits strange screening properties which arise because of a combination of metallic screening due to intraband transitions and insulating screening due to interband transitions; that all ultimately stems from the chiral relativistic dispersion relation [19].

3.3.2 Conductivity as a Function of Temperature

In this section, we reports our numerical results on σ of Graphene system as a function of temperature calculated using Eq. (3.1). Temperature dependent σ is very important quantity

which is directly measured in experiments. Moreover this quantity also shows at what temperature range systems have metallic or semiconducting nature. We first report temperature dependent σ of MLG and BLG in subsection (a). We also show how opening of energy gap in the MLG band structure changes the temperature dependent σ describe in the next subsection (b).

(a) Temperature Dependent Conductivity of MLG & BLG

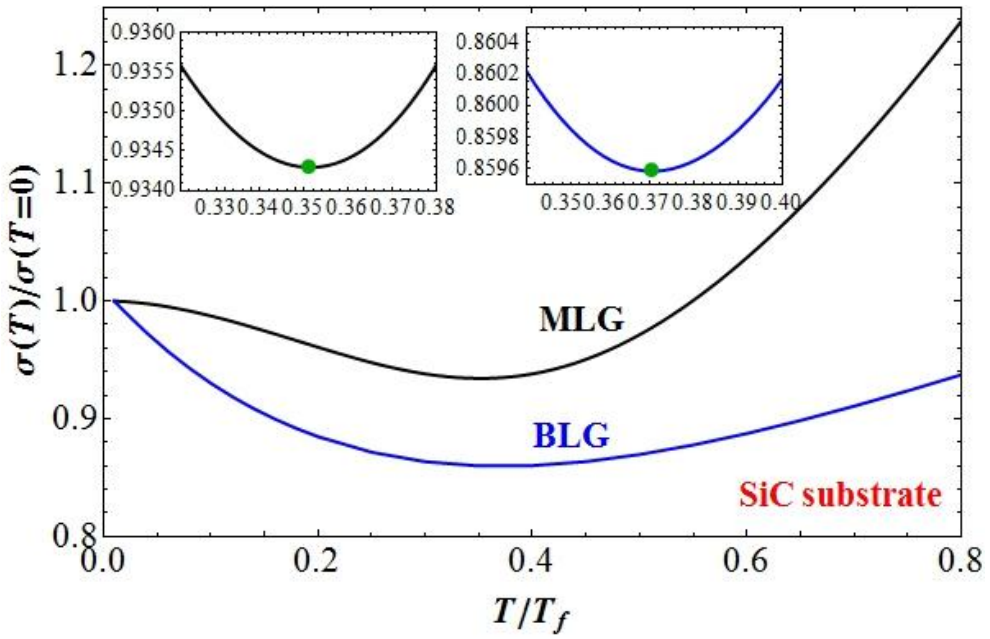

Figure 3.6: Numerically calculated temperature dependent conductivity of MLG (black) and BLG (blue) for both Graphene systems are on SiC substate where $\alpha = 1$ and $\beta = 4.3$. The light green spot in insets show minimum value of σ. Here we used $N = 1$.

Figure 3.6 shows the comparative numerical results of temperature dependent σ of MLG and BLG as a function of normalized temperature (T/T_f). Initially, for $T \ll T_f$, both the systems show metallic temperature dependent behaviors with different strengths. MLG has poor quadratic temperature dependence while BLG has strong linear temperature dependence. Change in nature of conduction, from metallic to semiconducting, takes place when $T \gtrsim 0.35T_f$ for MLG and $T \gtrsim 0.37T_f$ for BLG, as clearly sheen by light green spot in inset of Figure 3.6. The nonmonotonicity of temperature dependent σ in both systems can be

understood from the temperature-dependent polarization function as shown in Figure 3.1 and Figure 3.2.

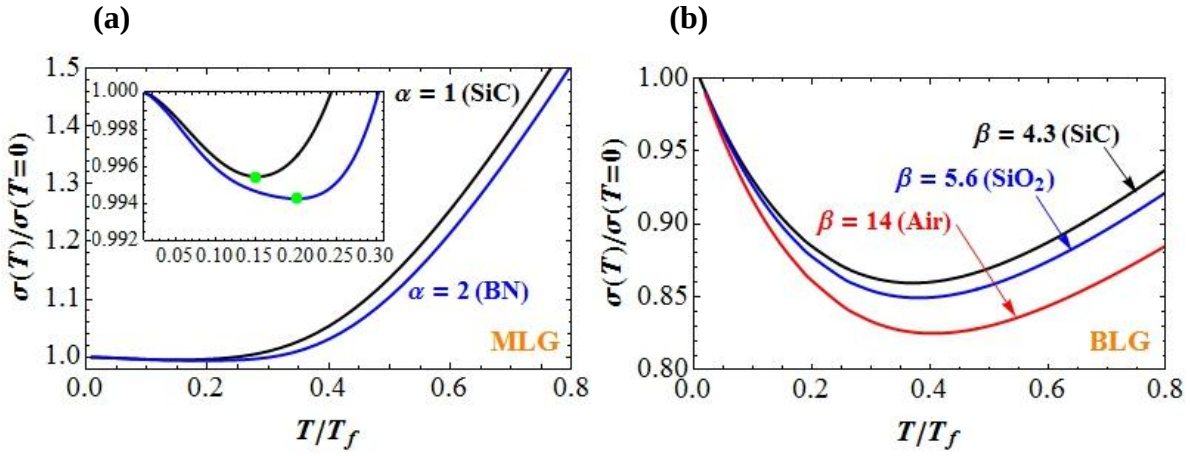

Figure 3.7: Numerically calculated σ as a function of normalized temperature (T/T_f) (a) for different values of $\alpha = 1$ & 2 corresponds to MLG on SiC (black) and BN (blue) and (b) for different values of $\beta = 4.3, 5.6$ & 14 corresponds to BLG on SiC (black), SiO_2 (blue) and Air (red). Here we used $N = 1$.

In Figure 3.7 we show our calculated σ as a function of temperature for different values of coupling constant, α and β for MLG and BLG respectively. α & β both are dependence on substrate. Moreover α is independent on carrier concentration while β is dependent on it. The small values of α and β indicate a weak-coupling system in terms of electron-electron interaction. As can be seen from Figure 3.7(a), in the low temperature limit temperature dependent σ decreases weakly quadratically with temperature, manifesting metallic behaviour, for both values of $\alpha = 1$ & 2 corresponds to MLG on SiC (black) and BN (blue). The strength of metallic behaviour decreases very slowly with increasing of α. We have also noted, from Figure 3.7(b), similar behavior in temperature dependent σ of BLG with relatively strong dependence on coupling constant due to the strong $q = 2k_f$ backward scattering occurring in this system. Substrates also change the local minimum of temperature dependent σ from $T \approx 0.15T_f$ for $\alpha = 1$ to $T \approx 0.2T_f$ for $\alpha = 2$ as can be seen from inset of Figure 3.7(a).

(b) Temperature Dependent Conductivity of MLGG

This section reports our results on energy averaged σ of MLGG as a function of temperature calculated using Eq. (3.1), which is then compared with that calculated at Fermi energy. It is found that when we incorporate the temperature dependence in dielectric function formalism, we observe significant difference between these two conductivities as function of temperatures. We thus find that it is grossly misleading to calculate temperature dependent σ at Fermi energy for comparison with experimental results. Our computed numerical results on normalized conductivity $\left(\sigma(T)/\sigma(T=0)\right)$ as a function of temperature, with the use of $1/\langle\tau\rangle$ and $1/\tau_{E_f}$, are plotted in Figures 3.8(a) to 3.8(d) for different values of a. The figures clearly demonstrate that the difference between two values of σ is insignificant only for temperatures very close to zero and the difference grows with increasing temperatures. For $a(=0, 0.3 \text{ \& } 0.6)$, $\sigma(T)/\sigma(T=0)$ using $1/\langle\tau\rangle$ initially remains almost constant and then it increases with temperature, which is not the case when $1/\tau_{E_f}$ used to compute $\sigma(T)/\sigma(T=0)$. A phase transition on changing temperature is also indicated by minimum values of σ computed using energy averaged and Fermi energy scattering rate for all values of gap, as can be seen from Figures 3.8(a) to 3.8(d). Elaborated behaviour of T verses $\sigma(T)/\sigma(T=0)$ near the transition point is shown insets of figures. The light green dot of curve indicates turning points of set curves.

(a)

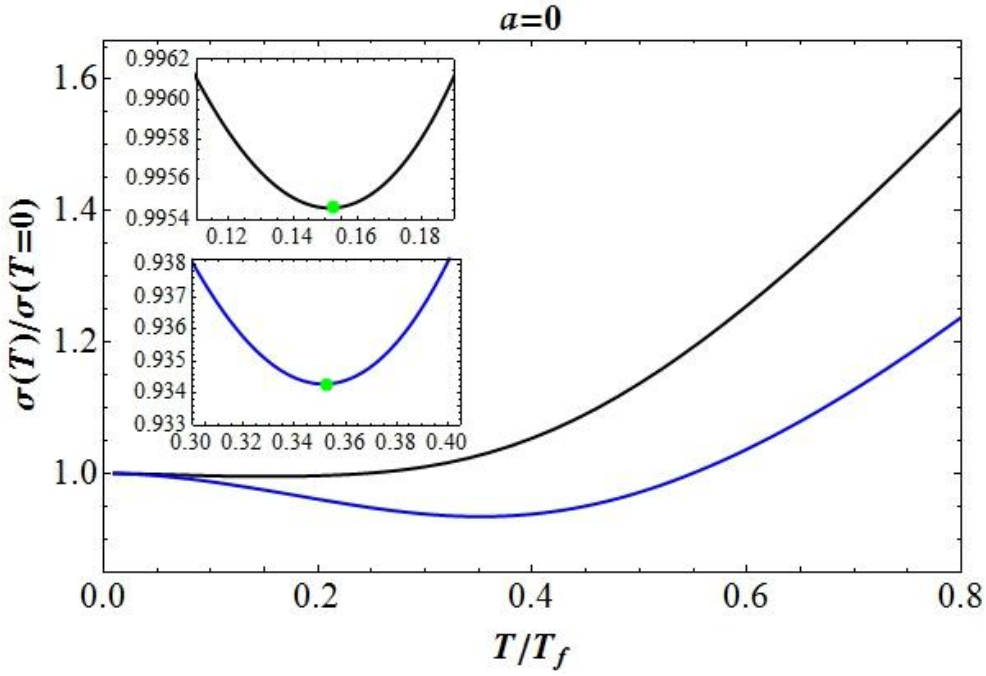
a=0
σ(T)/σ(T=0)
T/T_f
0.0
0.2
0.4
0.6
0.8
1.0
1.2
1.4
1.6
0.9962
0.9960
0.9958
0.9956
0.9954
0.12
0.14
0.16
0.18
0.938
0.937
0.936
0.935
0.934
0.933
0.30
0.32
0.34
0.36
0.38
0.40

(b)

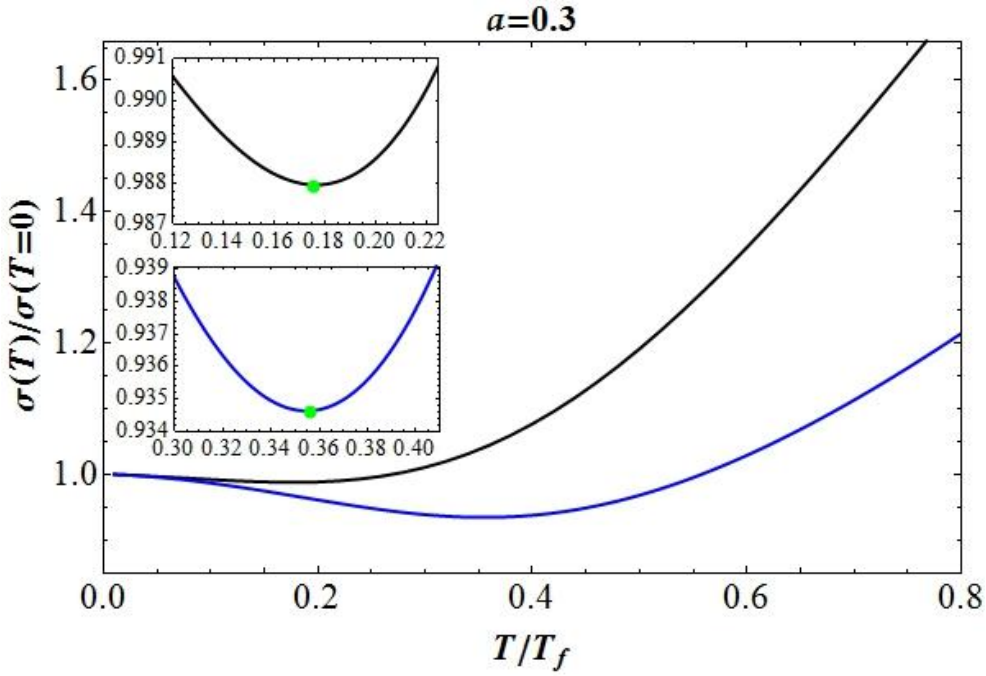
a=0.3
σ(T)/σ(T=0)
T/T_f
0.0
0.2
0.4
0.6
0.8
1.0
1.2
1.4
1.6
0.991
0.990
0.989
0.988
0.987
0.12
0.14
0.16
0.18
0.20
0.22
0.939
0.938
0.937
0.936
0.935
0.934
0.30
0.32
0.34
0.36
0.38
0.40

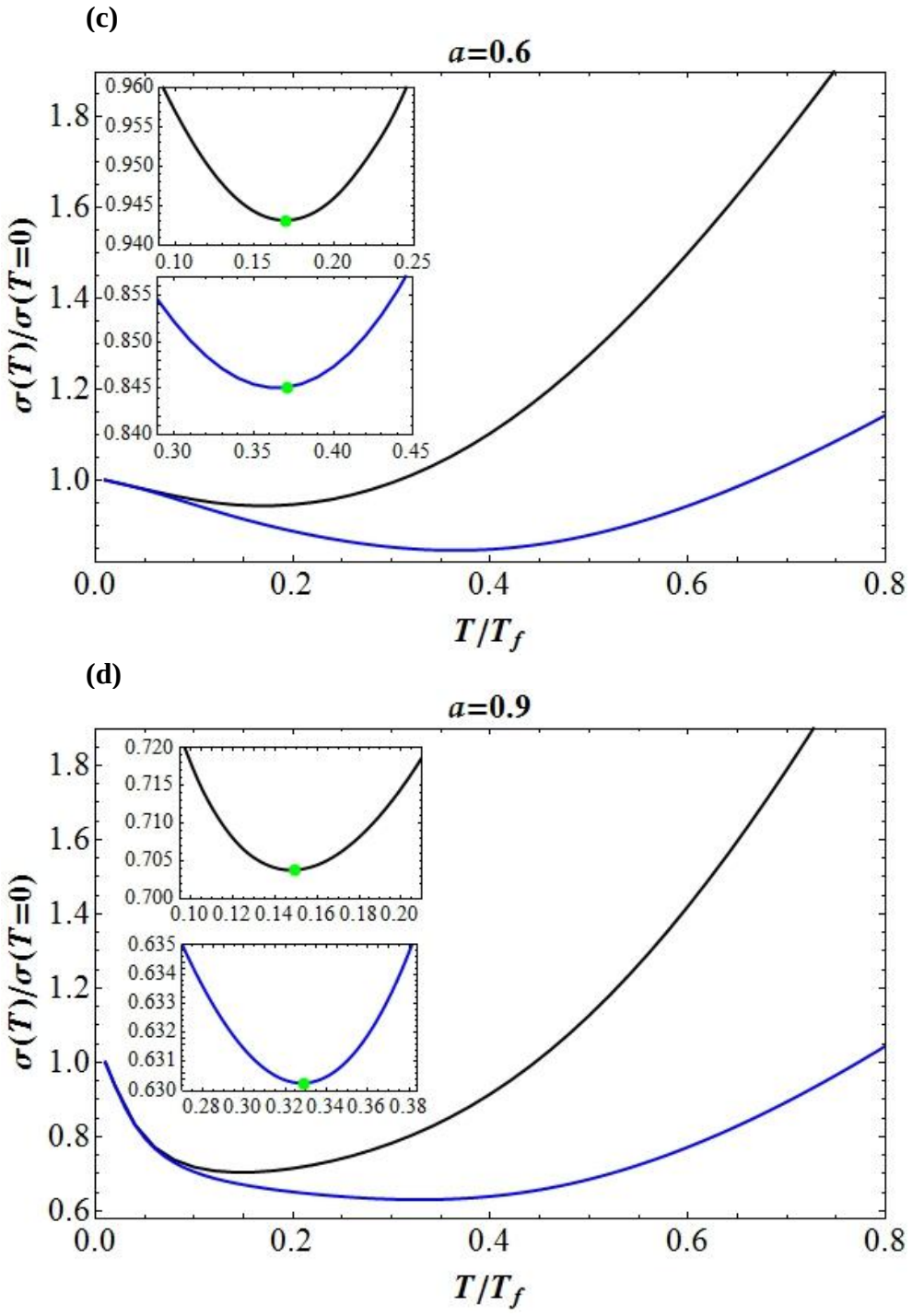

Figure 3.8: Conductivity as a function of temperature calculated at Fermi energy (solid blue line) and at average energy (solid black line) for different gap values; (a) $a = 0$, (b) $a = 0.3$, (c) $a = 0.6$ and (d) $a = 0.9$. Here we used coupling constant, $\alpha = 1$ (for SiC). The light green spot in insets show minimum value of σ. Here we used $N = 1$.

Change in nature of conduction calculated at average energy (Fermi energy), from poor conductor to semiconductor, takes place when $T \gtrsim 0.35T_f$ $\left(T \gtrsim 0.17T_f\right)$ for $a(=$

$0, 0.3, 0.6$ & 0.9). Strikingly opposite behaviour of σ with temperature in low and high temperature regimes is indicative of phase transition that can be obtained by selecting appropriate values of a and T in MLGG. Curves exhibit a minimum at $T \approx 0.35T_f$ and the change from poor metallic nature for $a(= 0, 0.3$ & $0.6)$ to good conductor nature at $a = 0.9$ in low temperature regime. The behaviour of the σ can be understood as follows; the increase in band gap reduces the σ in low temperature regime due to electron has insufficient excitation energy to jump from valance band to conduction band but increase in temperature increases the excitations and hence the raises the magnitude of σ. The Figure 3.9(a) showing the variation of σ with bandgap at different temperatures, corroborates the above behaviour. In Figure 3.9(b) shows the variation of σ as a function of temperature for $\alpha = 2$ which corresponds to Graphene on BN (Boron Nitride) substrate. The higher values of α indicate a strong coupling in terms of electron-electron interaction. A slight change (decrease) in nature of σ versus temperature curve can be noticed on enhancing coupling constant, α, from 1 to 2.

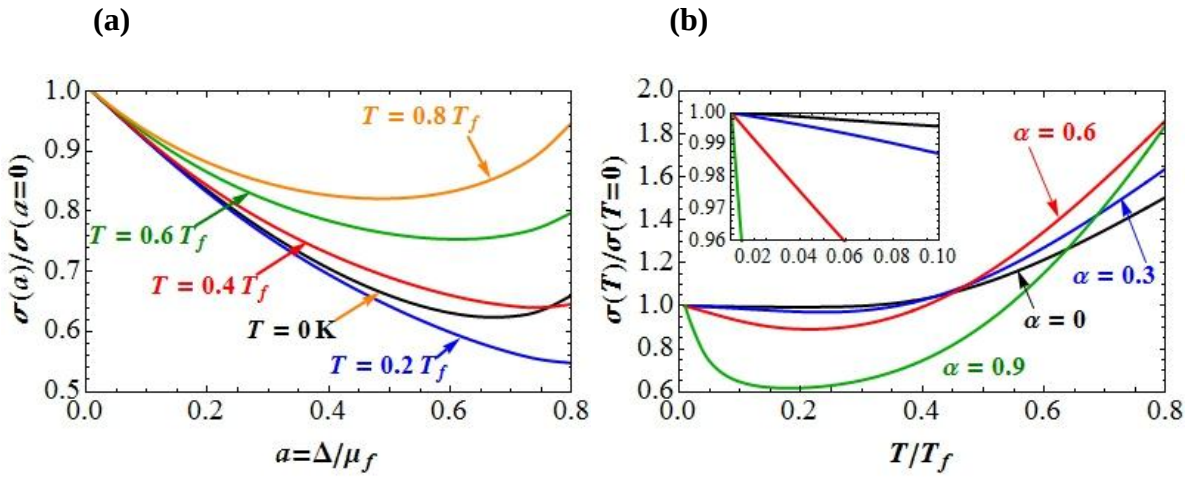

Figure 3.9: Conductivity (a) as a function of band gap for different values of temperature $T(= 0\text{ K}, 0.2T_f, 0.4T_f, 0.6T_f$ & $0.8T_f)$, using $\alpha = 1$, (b) as a function of temperature calculated at average energy for different gap values gap $a(= 0, 0.3, 0.6$ & $0.9)$ with coupling constant, $\alpha = 2$. Here we used $N = 1$.

3.3.3 Conductivity as a Function of Carrier Concentration

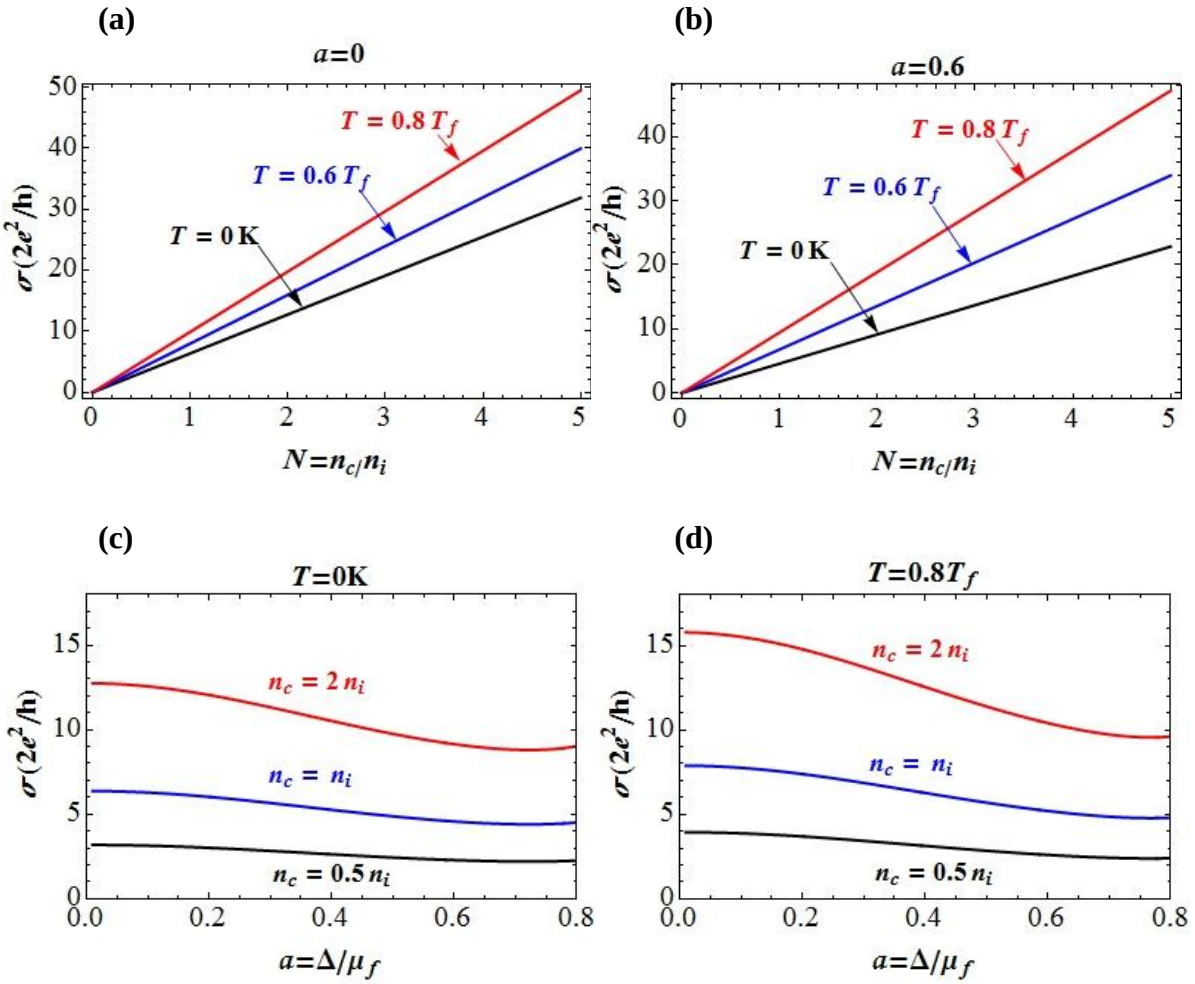

Figure 3.10: Conductivity as (i) a function of $N = n_c/n_i$ for different temperatures of $T(= 0\text{ K}, 0.6T_f \text{ \& } 0.8T_f)$ with gap values; (a) $a = 0$, (b) $a = 0.6$, (ii) a function of bandgap for $N(= 0.5, 1 \text{ \& } 2)$ at (c) $T = 0$ K and (d) $T = 0.8T_f$.

Our computed σ of MLGG using Eq. (3.1) as a function of carrier concentration, n_c at different temperatures is plotted in Figures 3.10(a) & 3.10(b) for two values of $a(= 0 \text{ \& } 0.6)$. Almost a linear enhancement of σ with n_c is seen for both values of a, similar to the experimentally observed behaviour in case of MLG [2]. Also the magnitude of σ increases with the increase in temperature. The Figures 3.10(c) & 3.10(d) depict the effect of variation of σ with band gap at $T = 0$ K and $T = 0.8T_f$, respectively, for three values of carrier concentration $N(= 0.5, 1.0 \text{ \& } 2.0)$. As can be noticed from the figure; this reconfirms that the

enhancement in the carrier concentration and temperature increases the σ whereas the increase in band gap reduces the σ.

3.5 References

[1] S. V. Morozov *et al.*, Phys. Rev. Lett. **100**, 016602 (2008).

[2] E. H. Hwang, S. Adam and S. D. Sarma, Phys. Rev. Lett. **98**, 186806 (2007).

[3] K. Nomura and A. H. Mac Donald, Phys. Rev. Lett. **98**, 076602 (2007).

[4] T. Ando, J. Phys. Soc. Jpn. **75**, 074716 (2006).

[5] K. Nomura and A. H. Mac Donald, Phys. Rev. Lett. **96**, 256602 (2006).

[6] V. V. Cheianov and V. I. Falko, Phys. Rev. Lett. **97**, 226801 (2006).

[7] Y. Zheng and T. Ando, Phys. Rev. B **65**, 245420 (2002).

[8] E. H. Hwang and S. D. Sarma, Phys. Rev. B **79**, 165404 (2009).

[9] M. Lv and S. Wan, Phys. Rev. B **81**, 195409 (2010).

[10] Y. W. Tan *et al.*, Eur. Phys. J. Spec. Top. **148**, 15 (2007).

[11] J. H. Chen *et al.*, Nat. Nanotechnol. **3**, 206 (2008).

[12] K. I. Bolotin *et al.*, Phys. Rev. Lett. **101**, 096802 (2008).

[13] W. Zhu *et al.*, Phys. Rev. B **80**, 235402 (2009).

[14] B. Feldman, J. Martin and A. Yacoby, Nat. Phys. **5**, 889(2009).

[15] K. Zou and J. Zhu, Phys. Rev. B **82**, 081407 (2010).

[16] S. G. Nam, D. K. Ki and H. J. Lee, Phys. Rev. B **82**, 245416 (2010).

[17] E. H. Hwang and S. D. Sarma, Phys. Rev. Lett. **101**, 156802 (2008).

[18] B. Wunsch *et al.*, New J. Phys. **8**, 318 (2006).

[19] E. H. Hwang and S. D. Sarma, Phys. Rev. B **75**, 205418 (2007).

[20] R. Sensarma, E. H. Hwang and S. D. Sarma, Phys. Rev. B **82**, 195428 (2010).

[21] K. Shiyuza, Phys. Rev. B **75**, 245417 (2007).

[22] A. Qaiumzadeh, R. Asgari, Phys. Rev. B **79**, 075414 (2009).

[23] P. K. Pyatkovskiy, J. Phys. Condens. Matt. **21**, 025506 (2009).

[24] J. N. Zhang, Phys. Scr. **83**, 035002 (2011).

[25] P. K. Pyatkovskiy and V. P. Gusynin Phys. Rev. B **83**, 075422 (2011).

[26] O. V. Gamayun, Phys. Rev. B **84**, 085112 (2011).

[27] A. Qaiumzadeh, R. Asgari, New. J. Phys. **11**, 095023 (2009).

[28] V. N. Kotov, V. M. Pereira, B. Uchoa, Phys. Rev. B **78**, 075433 (2008).

[29] A. Scholz, J. Schliemann, Phys. Rev. B **83**, 235409 (2011).

[30] F. Stern, Phys. Rev. Lett. **44**, 1469 (1980).

[31] S. D. Sarma, Phys. Rev. B **33**, 5401 (1986).